

Ultrafast Photosensitization of Phthalocyanines through Their Axial Ligands

William Rodríguez-Córdoba,[†] Raquel Noria, César A. Guarín, and Jorge Peon*

Instituto de Química, Universidad Nacional Autónoma de México, Circuito Exterior, Ciudad Universitaria, México, 04510, D.F., México

S Supporting Information

ABSTRACT: We have studied the energy transfer properties of a novel silicon phthalocyanine that coordinates two anthracene-9-carboxylate groups in the form of trans axial ligands. Our objectives were to generate a system with auxiliary chromophores that enhance the light absorption properties of the macrocycle in a specific region in the UV and to evaluate the efficiency and time scales for energy transfer. The ligand coordination through a carboxylate group directly attached to the anthracenic system allows for close proximity of the donor and acceptor chromophores. The energy transfer process was observed to be nearly 100% efficient and to occur on a time scale of 370 fs. From the energy relations of the donor and acceptor states and the observed dynamics, the initial energy transfer step is likely to involve upper electronic states of the phthalocyanine rather than the states of the lowest-energy vibroelectronic Q bands.

The indirect electronic excitation of a molecular system through auxiliary chromophores is of great importance for light-harvesting applications. For example, the action spectrum of natural photosynthetic systems is expanded by the presence of different supplementary pigments.¹ Phthalocyanines are macrocyclic aromatic molecules with broad applications that involve light absorption, including solar cells,² photodynamic therapy,^{3,4} chemiresistors,⁵ information storage,⁶ photocatalysis for synthetic or degradation purposes,^{7,8} etc. The ability to photoexcite this kind of molecule indirectly through an auxiliary chromophore can have significant importance because this kind of sensitization would improve their light-absorbing capacities in specific regions of the spectrum. The applications could range from high-density data storage using UV light of a particular frequency beyond the B-band system to light detection through secondary fluorescence or two-photon sensitization for photodynamic therapies. In addition to augmenting their photoabsorption properties (as shown in this communication), the bonding of axial ligands to silicon phthalocyanines provides them with a significantly improved solubility, as these bulky substituents impede the formation of aggregates through π -stacking interactions.^{9–12} Their tendency to stay as monomeric units also causes axially substituted phthalocyanines to have significantly higher emission quantum yields and sharper absorption and emission transitions in the UV–vis region, even at high concentrations.¹³

In this communication, we show that polyaromatic systems bonded directly through a carboxylate group to a silicon

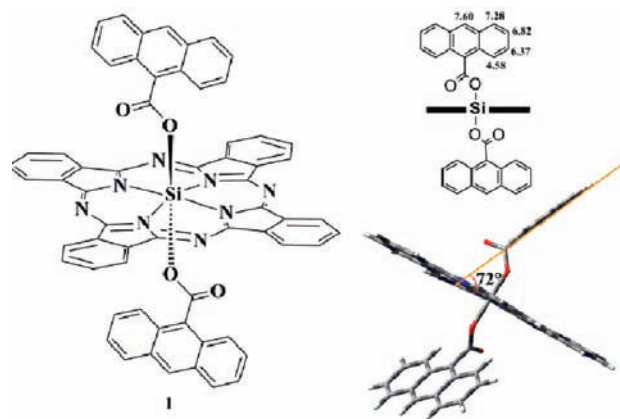


Figure 1. (left) Molecular structure of the anthracene-9-carboxylate axially disubstituted phthalocyanine of this study. (top right) Scheme of the chemical displacement ¹H NMR assignments. (right bottom) Model for this structure calculated using the PM6 theoretical method.

phthalocyanine in the form of trans axial ligands induce secondary excitation of the macrocycle through 100% efficient, sub-picosecond, irreversible energy transfer, even when the spectral overlap between the Q system and the ligand emission is minimal (see below). Although the syntheses of several axially disubstituted phthalocyanines have been reported,^{14–20} this is to the best of our knowledge the first communication reporting direct studies of the macrocycle's sensitization through a polycyclic aromatic ligand, which drastically enhances the system's light-absorption properties with an effective additional band in the UV region.

The silicon phthalocyanine (SiPc) bis(anthracene-9-carboxylate) compound **1** (Figure 1) was synthesized through nucleophilic displacement of two chloride substituents from the dichlorinated silicon phthalocyanine PcSiCl₂ by reaction with anthracene-9-carboxylic acid in toluene solution. This substituent was chosen on the basis of the consideration that the anthracene moiety has excitations with well-defined transition moments, which (as will be shown) allows the mechanistic assessment of the energy transfer process. The identity of compound **1** was established by various spectroscopic methods, including ¹H NMR, IR, and UV–vis spectroscopy, MALDI–TOF mass spectrometry, and elemental analysis. In particular, the shielding effects on the ¹H NMR signals of the axial ligands from the ring currents allowed the structure to be clearly discerned: From the isoshielding zones, the protons at the ligands' 1 and 8 positions (a doublet)

Received: December 16, 2010

Published: March 10, 2011

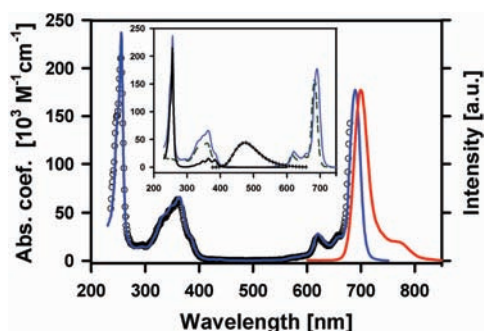


Figure 2. UV-vis absorption (blue line), emission (red line), and excitation (black \circ) spectra of **1**. For the emission and excitation spectra, the excitation and detection wavelengths were 385 and 700 nm, respectively. Inset: Absorption spectra of **1** (blue line), anthracene-9-carboxylic acid (black line, $\times 2$), and myristate trans-disubstituted silicon phthalocyanine (green dashed line) and the emission spectrum of free anthracene-9-carboxylic acid (black $+$). Solutions were prepared in CH_2Cl_2 .

were drastically upfield-shifted to δ 4.58 (4H). Similarly, the protons at the 2 and 7 positions (a doublet) were shifted to δ 6.37 (4H), and those at the 3 and 6 positions appeared at δ 6.82, while those at the 4 and 5 positions showed up at δ 7.28. Finally, the proton at the 10 position corresponded to a singlet signal at δ 7.60. Full characterization is included in the Supporting Information (SI).

The optical spectra of compound **1** are shown in Figure 2, where we have also included the absorption spectrum of the ligand derivative anthracene-9-carboxylic acid and that of a reference silicon phthalocyanine with myristate chains as trans axial ligands.^{11,12} In the inset of Figure 2, we have also included the emission spectrum of anthracene-9-carboxylic acid, which was taken as a model for the ligand fluorescence. As reported previously, the carboxylic group causes the emission band of the acid to be totally unstructured and centered at 480 nm.²¹ Also, it is clear that the spectral overlap with the phthalocyaninic absorption **1** is minimal and practically occurs only at the red edge of the emission, where it coincides with the shorter-wavelength vibronic bands of the Q system around 600 nm.

As can be seen, the absorption spectrum of **1** can be viewed as the superposition of the spectrum of the myristate silicon macrocycle and that of the axial ligands. In particular, at 257 nm, where the ligand shows the typical strong absorption due to the $S_0 \rightarrow S_3$ anthracenic transition, the absorption coefficient for **1** coincides (within 10%) with the arithmetic addition of the coefficient for the free ligand multiplied by 2 and the coefficient for the macrocycle (taken from the trans myristate silicon phthalocyanine in the same solvent). This consideration contributes to the elucidation of the structure (2:1 ligand:macrocycle relation) and furthermore indicates that the two chromophores are independent and practically unperturbed aromatic systems. It is noteworthy that in **1** the absorption coefficient at 257 nm is $237 \times 10^3 \text{ M}^{-1} \text{ cm}^{-1}$, while in the myristate silicon phthalocyanine it is only $15 \times 10^3 \text{ M}^{-1} \text{ cm}^{-1}$.

The emission spectrum of **1** shows only the phthalocyanine-type band system centered at 705 nm, congruent with a highly efficient energy transfer channel that is independent of excitation wavelength (see below). The corrected excitation spectrum of **1** matches the absorption spectrum, which demonstrates that even though the anthracenic and phthalocyanine-type chromophores have different relative contributions across the spectrum, the emission yield is

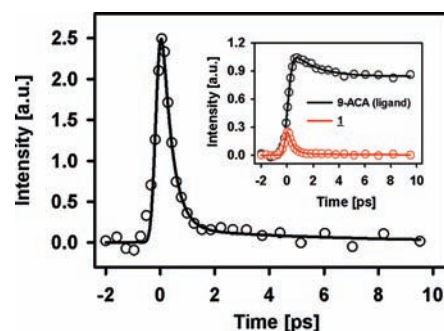


Figure 3. Results of femtosecond-resolved fluorescence up-conversion experiments on **1** in CH_2Cl_2 solution. Inset: Comparison between the results for solutions of anthracene-9-carboxylic acid (9-ACA, black) and **1** (red). Excitation wavelength = 385 nm; fluorescence wavelength = 480 nm.

nearly independent of the excitation wavelength. In fact, measurements of the emission quantum yield at three different excitation frequencies yielded the same values within the experimental uncertainties: $\phi_{\text{fluor}}(\lambda_{\text{exc}} = 300 \text{ nm}) = 0.27 \pm 0.02$, $\phi_{\text{fluor}}(\lambda_{\text{exc}} = 385 \text{ nm}) = 0.30 \pm 0.01$, and $\phi_{\text{fluor}}(\lambda_{\text{exc}} = 580 \text{ nm}) = 0.28 \pm 0.01$. Only when **1** was excited below 280 nm did we see a more than 10% mismatch between the excitation and absorption spectra (normalized at the vibronic bands around 600 nm). This probably indicates that extra decay channels make small contributions upon excitation to the higher-lying electronic states of the ligand.

Figure 3 shows the results of femtosecond fluorescence up-conversion measurements on **1** in CH_2Cl_2 under magic-angle conditions with an excitation wavelength of 385 nm and detection at 480 nm (fluorescence). Importantly, from the absorption spectra of **1** and its components, we estimate that at this pump wavelength the absorbance is due primarily to ligand excitation, with a $< 25\%$ contribution from absorbance by the macrocycle. The detection wavelength for the measurements in Figure 3 lies at the center of the emission band of the free ligand. This anthracenic emission decays on a subpicosecond time scale with a single exponential decay time of 370 fs. In the inset of Figure 3, we have also shown a comparison between the time-resolved emission of **1** and that of a solution of anthracene-9-carboxylic acid. As can be seen, in the “ligand-only” result, the emission decays with a much longer lifetime (besides the ultrafast modulations due to solvent relaxation; see the SI). This comparison emphasizes the fact that the excited states localized at the ligand decay several orders of magnitude faster than those in the “free” ligand, which shows a long decay component of 7.5 ns (fluorescence lifetime). This is the most prominent signature of the highly efficient energy transfer channel and is again consistent with the fact that no anthracenic emission was observed in the steady-state fluorescence spectrum.

The respective measurements with 690 to 710 nm detection are shown in Figure 4. These signals, coming from the phthalocyanine system, actually show an instantaneous appearance followed by a 20 ps rise-time component across the fluorescence spectrum, as shown in the main plot and the insets. Such a rise behavior can be considered as characteristic of the accumulation of the population of the vibrationally relaxed phthalocyaninic S_1 state on the basis of the observation that the myristate phthalocyanine shows a 14 ps rise (690 nm detection) when excited in the Soret band (see the SI).

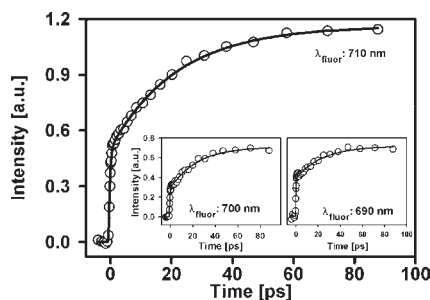


Figure 4. Results of femtosecond-resolved fluorescence up-conversion experiments on **1** in CH_2Cl_2 solution.

The rise behavior in compound **1** is followed by the lifetime decay of 4.1 ns (data shown in the SI). Since the 20 ps component occurs at all of the wavelengths of the Q system with the same time constant, it is unlikely that the rise behavior implies a spectral reshaping from vibrational relaxation within the first singlet excited state. The possible involvement of upper electronic states in the energy transfer step is discussed below.

In order to gain some insights into the molecular structure and how it relates to the energy transfer mechanism, we performed geometry optimizations at several levels of theory, including Hartree–Fock (HF), density functional theory (DFT), and semiempirical PM6, using the Gaussian 09 suite of programs.²² Specifically, these calculations provided estimates of critical structural parameters for the prediction of energy transfer rate constants for the Förster-type mechanism. Both the HF and DFT methods employed the 6-311G(d,p) basis set, and the DFT calculations considered the PBE0 functional with and without the polarizable continuum model to account for the CH_2Cl_2 solvent.^{23,24}

In the Förster model (Coulombic through-space dipole–dipole interactions), the important geometric factors are the donor–acceptor (D–A) distance, R , and the orientation factor, $\Gamma = \cos(\theta_{\text{DA}}) - 3 \cos(\theta_{\text{D}}) \cos(\theta_{\text{A}})$, which is calculated from the angle between the transition dipole moments (θ_{DA}) and their angles with respect to the vector connecting the D and A centers (θ_{D} and θ_{A} , respectively). In our system, the donor $S_0 \leftarrow S_1$ transition lies along the short axis of the anthracenic systems, and the optimized geometries from our calculations show that the polyaromatic rings are slightly tilted toward the macrocycle, as shown in Figure 1 ($\theta_{\text{DA}} = 72\text{--}78^\circ$, depending on the method). This structural feature is due to the bonding mode through one of the oxygens in the carboxylic group, where the CO_2 triad is actually not coplanar with the anthracenic rings in this kind of system.²⁵

Using the optimized geometries together with the spectroscopic data in Figure 2, we estimated that the Förster rate constants vary from $6.91 \times 10^{12} \text{ s}^{-1}$ ($k_{\text{ET}}^{-1} = 145 \text{ fs}$) with the PM6 method to $4.78 \times 10^{12} \text{ s}^{-1}$ ($k_{\text{ET}}^{-1} = 210 \text{ fs}$) for the HF method (for details, see the Supporting Information). Notably, these rates are actually higher than that of the observed 370 fs decay of the donor fluorescence. Such a discrepancy could relate to a failure of the simple Förster model for such short D–A distances ($R \approx 5.4 \text{ \AA}$), where, among other things, multipole interactions would have to be included. However, our calculations emphasize the fact that given the close D–A distance, the small tilt angle of the anthracenic unit is enough to ensure ultrafast energy transfer.

Although we estimate that the Förster-type energy transfer mechanism is enough to guarantee ultrafast energy transfer, the

actual process may very well simultaneously occur through the electron exchange mechanism (Dexter process), given that the 480 nm decay and the 680–720 nm signal evolution (20 ps rise component) do not show a one-to-one correspondence. This observation implies that the excitation transfer events are likely to involve upper electronic states of the phthalocyanine system acting as intermediary or receiver states that precede the 20 ps accumulation of the fully relaxed phthalocyaninic S_1 state. Since the Dexter mechanism, which operates only at short distances, requires overlap of the D and A electronic wave functions, we verified that such overlap is not negligible for our system. From comparisons between the atom-to-atom distances (R) and the sum of their van der Waals radii (L), we conclude that the factor of $\exp(-2R/L)$ in the expression for the transfer rate constant in the Dexter mechanism can be significant, with R/L ratios near unity for several atom pairs. Additionally, the isosurfaces of near-frontier molecular orbitals from the theoretical calculations show that in particular at the carboxylate group, the first few virtual molecular orbitals centered at the ligand (necessarily involved in donor excitation) have a non-negligible contact with frontier orbitals localized at the macrocycle, in particular at the axial bonding site. Details about these estimations are included in the SI.

It is interesting also to compare the energy transfer properties of compound **1** with those of the free-base porphyrin–zinc phthalocyanine dyads recently reported by Maligaspe et al.,²⁶ which were similarly assembled via axial coordination and where the energy transfer times range from 2 to 25 ps. In these dyads, the free-base tetraphenylporphyrin (donor) and the phthalocyanine (acceptor) are linked by an imidazole bridge that joins the two chromophores through the phthalocyanine’s central metal, defining center-to-center distances of 7–13 Å. Such distances are somewhat longer than the center-to-center distance in compound **1** ($\approx 5.4 \text{ \AA}$; see the SI), which in part explains the different time scales (subpicosecond energy transfer for **1**). It should also be mentioned that the electronic structure calculations included in ref 26 showed that no direct electronic communication is expected for the dyads. In contrast, for compound **1**, some D–A orbital overlap can be distinguished, as mentioned previously, which may allow the contribution of an electron-exchange-type mechanism to the energy transfer rate, possibly involving upper electronic states of the macrocycle. We emphasize that such close contact between the donor and acceptor moieties can be accomplished only through a binding mode like that in **1**, which involves a carboxylate group that is directly conjugated with the anthracenic aromatic system.

In conclusion, we have reported that when polycyclic aromatic systems are bonded directly to the central atom of a silicon phthalocyanine as axial substituents through a carboxylate group, the macrocycle can be indirectly excited through light absorption by the ligands. The energy transfer process has been demonstrated to occur with nearly 100% efficiency across most of the spectrum on time scales of a few hundred femtoseconds. The time scale for the excitation transfer event implies that there are practically no competing processes such as intersystem crossing or ground-state recovery. The sensitization of these molecules with axial chromophores with intense and well-defined transitions at wavelengths shorter than the B-band system implies that the phthalocyanine can be excited with an effective absorption coefficient of more than $230 \times 10^3 \text{ M}^{-1} \text{ cm}^{-1}$ in the UV region. Foreseen applications include high-density data storage with UV light.

■ ASSOCIATED CONTENT

S Supporting Information. Experimental procedures, Förster transfer rate calculations, details of geometry optimizations, additional time-resolved data, atomic coordinates, orbital depictions, and complete ref 22. This material is available free of charge via the Internet at <http://pubs.acs.org>.

■ AUTHOR INFORMATION

Corresponding Author

jpeon@servidor.unam.mx

Present Addresses

[†]Department of Chemistry, Emory University, Atlanta, Georgia 30322.

■ ACKNOWLEDGMENT

For financial support, we thank CONACyT (Grant 79494) and PAPIIT-UNAM (Grant IN 204211). For computational resources, we thank DGSCA-UNAM.

■ REFERENCES

- (1) Hu, X.; Schulten, K. *Phys. Today* **1997**, *50*, 28.
- (2) Morandeira, A.; Lopez-Duarte, I.; O'Regan, B.; Martinez-Diaz, M. V.; Forneli, A.; Palomares, E.; Torres, T.; Durrant, J. R. *J. Mater. Chem.* **2009**, *19*, 5016.
- (3) Camerin, M.; Magaraggia, M.; Soncin, M.; Jori, G.; Moreno, M.; Chambrier, I.; Cook, M. J.; Russell, D. A. *Eur. J. Cancer* **2010**, *46*, 1910.
- (4) Li, H.; Nguyen, N.; Fronczek, F. R.; Vicente, M. G. H. *Tetrahedron* **2009**, *65*, 3357.
- (5) Shu, J. H.; Wickle, H. C.; Chin, B. A. *Sens. Actuators, B* **2010**, *148*, 498.
- (6) Chen, W.; Wee, A. T. S. *J. Phys. D: Appl. Phys.* **2007**, *40*, 6287.
- (7) Zanjanchi, M. A.; Ebrahimian, A.; Arvand, M. *J. Hazard. Mater.* **2010**, *175*, 992.
- (8) Salinas-Guzman, R. R.; Guzman-Mar, J. L.; Hinojosa-Reyes, L.; Peralta-Hernandez, J. M.; Hernandez-Ramirez, A. *J. Sol-Gel Sci. Technol.* **2010**, *54*, 1.
- (9) Beltran, H. I.; Esquivel, R.; Sosa-Sanchez, A.; Sosa-Sanchez, J. L.; Hopfl, H.; Barba, V.; Farfan, N.; Garcia, M. G.; Olivares-Xometl, O.; Zamudio-Rivera, L. S. *Inorg. Chem.* **2004**, *43*, 3555.
- (10) Beltran, H. I.; Esquivel, R.; Lozada-Cassou, M.; Dominguez-Aguilar, M. A.; Sosa-Sanchez, A.; Sosa-Sanchez, J. L.; Hopfl, H.; Barba, V.; Luna-Garcia, R.; Farfan, N.; Zamudio-Rivera, L. S. *Chem.—Eur. J.* **2005**, *11*, 2705.
- (11) Sosa-Sanchez, J. L.; Sosa-Sanchez, A.; Farfan, N.; Zamudio-Rivera, L. S.; Lopez-Mendoza, G.; Flores, J. P.; Beltran, H. I. *Chem.—Eur. J.* **2005**, *11*, 4263.
- (12) Sosa-Sanchez, J. L.; Galindo, A.; Gnecco, D.; Bernes, S.; Fern, G. R.; Silver, J.; Sosa-Sanchez, A.; Enriquez, R. G. *J. Porphyrins Phthalocyanines* **2002**, *6*, 198.
- (13) Nyokong, T. *Coord. Chem. Rev.* **2007**, *251*, 1707.
- (14) Maree, M. D.; Kuznetsova, N.; Nyokong, T. *J. Photochem. Photobiol., A* **2001**, *140*, 117.
- (15) Fujitsuka, M.; Ito, O.; Konami, H. *Bull. Chem. Soc. Jpn.* **2001**, *74*, 1823.
- (16) Silver, J.; Sosa-Sanchez, J. L.; Frampton, C. S. *Inorg. Chem.* **1998**, *37*, 411.
- (17) Farren, C.; Christensen, C. A.; FitzGerald, S.; Bryce, M. R.; Beeby, A. *J. Org. Chem.* **2002**, *67*, 9130.
- (18) Farren, C.; FitzGerald, S.; Bryce, M. R.; Beeby, A.; Batsanov, A. S. *J. Chem. Soc., Perkin Trans. 2* **2002**, 59.
- (19) Barker, C. A.; Findlay, K. S.; Bettington, S.; Batsanov, A. S.; Perepichka, I. F.; Bryce, M. R.; Beeby, A. *Tetrahedron* **2006**, *62*, 9433.
- (20) Pelliccioli, A. P.; Henbest, K.; Kwag, G.; Carvagno, T. R.; Kenney, M. E.; Rodgers, M. A. J. *J. Phys. Chem. A* **2001**, *105*, 1757.
- (21) Momiji, I.; Yoza, C.; Matsui, K. *J. Phys. Chem. B* **2000**, *104*, 1552.
- (22) Frisch, M. J.; et al. *Gaussian 09*; Gaussian, Inc.: Wallingford, CT, 2009.
- (23) Adamo, C.; Barone, V. *Chem. Phys. Lett.* **1999**, *314*, 152.
- (24) Cossi, M.; Barone, V. *J. Chem. Phys.* **2001**, *115*, 4708.
- (25) Plaza-Medina, E. F.; Rodriguez-Cordoba, W.; Morales-Cueto, R.; Peon, J. *J. Phys. Chem. A* **2011**, *115*, 577.
- (26) Maligaspe, E.; Kumpulainen, T.; Lemmetyinen, H.; Tkachenko, N. V.; Subbaiyan, N. K.; Zandler, M. E.; D'Souza, F. J. *Phys. Chem. A* **2010**, *114*, 268.